

AperTO - Archivio Istituzionale Open Access dell'Università di Torino

## Evaluating the relevance of sequence conservation in the prediction of pathogenic missense variants

### This is the author's manuscript

*Original Citation:*

*Availability:*

This version is available <http://hdl.handle.net/2318/1844320> since 2022-02-28T16:00:05Z

*Published version:*

DOI:10.1007/s00439-021-02419-4

*Terms of use:*

Open Access

Anyone can freely access the full text of works made available as "Open Access". Works made available under a Creative Commons license can be used according to the terms and conditions of said license. Use of all other works requires consent of the right holder (author or publisher) if not exempted from copyright protection by the applicable law.

(Article begins on next page)

# Evaluating the relevance of sequence conservation in the prediction of pathogenic missense variants

*Emidio Capriotti<sup>1\*</sup> and Piero Fariselli<sup>2\*</sup>*

<sup>1</sup>*BioFold Unit, Department of Pharmacy and Biotechnology (FaBiT), University of Bologna,  
Via F. Selmi 3, 40126 Bologna, Italy.*

<sup>2</sup>*Department of Medical Sciences, University of Torino,  
Via Santena 19, 10126, Torino, Italy.*

Contacts: [emidio.capriotti@unibo.it](mailto:emidio.capriotti@unibo.it), [piero.fariselli@unito.it](mailto:piero.fariselli@unito.it)

## Abstract

Evolutionary information is the primary tool for detecting functional conservation in nucleic acid and protein. This information has been extensively used to predict structure, interactions and functions in macromolecules. Pathogenicity prediction models rely on multiple sequence alignment information at different levels. However, most accurate genome-wide variant deleteriousness ranking algorithms consider different features to assess the impact of variants. Here, we analyze three different ways of extracting evolutionary information from sequence alignments in the context of pathogenicity predictions at DNA and protein levels. We showed that protein sequence-based information is slightly more informative in the annotation of Clinvar missense variants than those obtained at the DNA level. Furthermore, to achieve the performance of state-of-the-art methods, such as CADD and REVEL, the conservation of reference and variant, encoded as frequencies of reference/alternate alleles or wild-type/mutant residues, should be included. Our results on a large set of missense variants show that a basic method based on three input features derived from the protein sequence profile performs similarly to the CADD algorithm which uses hundreds of genomic features. *As expected, our method results in ~3% lower area under the receiver operating characteristic curve (AUC) when compared with an ensemble-based algorithm (REVEL). Nevertheless, the combination of predictions of multiple methods can help to identify more reliable predictions.* These observations indicate that for missense variants, evolutionary information, when properly encoded, plays the primary role in ranking pathogenicity.

**Keywords:** Variant interpretation, Pathogenic missense variants, Evolutionary information, Conservation score

## Introduction

High-throughput sequencing technologies have changed our daily research by rapidly accumulating genomic data and helping to profile patient genomes (MacArthur et al. 2014; Claussnitzer et al. 2020) . These studies make variant interpretation a fundamental challenge in precision medicine (Fernald et al. 2011; Capriotti et al. 2012; McInnes et al. 2021). Missense variants by changing a single amino acid in a protein sequence can be neutral or induce loss of function.

In the last two decades several methods have been developed to prioritize functional missense variants relying on protein sequence/structure information (Tennessen et al. 2012; Niroula and Vihinen 2016; Ancien et al. 2018; Petrosino et al. 2021) and the protein interaction networks (Rost et al. 2016; Capriotti et al. 2019; Ozturk and Carter 2021).

It is widely accepted that evolutionary information encoded in multiple sequence alignments of DNAs and proteins is a major resource for scoring variant pathogenicity. Several methods for scoring the nucleotide and amino acid conservation have been defined (Schneider 1997; Valdar 2002). Although there is no rigorous test for judging a conservation measure, in general, quantitative conservation measures are site-specific scores calculated from a vector representing the relative frequency of the amino acids or nucleotides in a given position of a multiple sequence alignment. Among the most commonly used scores are those calculating the Euclidean distance between two sets of amino acid frequencies (Valdar 2002) and Shannon's information-theoretic entropy (Capra and Singh 2007). Such site-specific scores, which are important for identifying functionally conserved regions, do not explicitly depend on the pairs of wild-type and mutant nucleotides/amino acids observed in a specific mutation process. For scoring the pathogenicity of a specific variation, we considered the most basic quantitative measures calculating the frequency of the wild-type and mutant nucleotides/residues in a given site.

This paper evaluates the relevance of this information for missense variant predictions by comparing simple scores and simple predictors with the widely used and well-performing Combined Annotation-Dependent Depletion (CADD) algorithm (Rentzsch et al. 2019) and REVEL (Ioannidis et al. 2016).

We computed the conservation scores on DNA (*PhastCons100way* and *PhyloP100way*), the frequencies of the reference and alternative alleles in the genome, and frequencies of the wild-type and mutant residues in protein multiple alignments. Our analysis showed that a machine learning method trained on a few sequence conservation features at DNA or protein levels, achieves similar performance of a state-of-the-art algorithm. In this work we compared the performance of CADD and REVEL with those reached by three different basic gradient boosting algorithms on a set of missense variants from the *Clinvar* database. Our result indicates that the evolutionary information provides the main features for scoring the pathogenicity of missense variants.

## Material and methods

### Datasets

To evaluate the performance of different machine learning methods for predicting the pathogenicity of missense variants we collected two datasets from the *Clinvar* database (Landrum et al. 2020). For building the two datasets we considered two versions of *Clinvar* released in June 2020 and August 2021, respectively. The first dataset (*CommonClinvar*) consists of the missense variants annotated as *Pathogenic* and *Benign* in both versions of the database while the second dataset (*NewClinvar*) collects the new missense variants reported in the last version of *Clinvar* since June 2020 (Fig. S1). The variants reported in the older version of *Clinvar* not confirmed in the last version were discarded. Thus, the *CommonClinvar* consists of 36,751 missense variants from 7,582 proteins 53.5% of which are annotated as *Benign* and the remaining ones (46.5%) as *Pathogenic*. *NewClinvar*, which includes only the newly annotated variants, is composed of 5,172 from 1,855 proteins 43.4% of which are reported as *Benign* and 56.6% as *Pathogenic*. The composition of the two datasets is summarized in Table S1. Both *CommonClinvar* and *NewClinvar* datasets are available as supplementary files.

### Conservation features

In this work we analyzed the performance in the prediction of pathogenic variants using three basic methods based on sequence conservation features. Each method considers only three input features, which are described below.

As a baseline we implemented a method considering two site-specific conservation scores (*PPScore*) calculated on a genome level multiple sequence alignment and made available through the UCSC genome browser (Kent et al. 2002). The conservation scores used in the first method are calculated by *PhastCons* (Siepel et al. 2005) and *PhyloP* (Pollard et al. 2010) algorithms.

In the second method (*DNAProf*), the frequencies of the reference and alternative alleles in the mutated site are calculated for each variant from the *multiz100way* multiple sequence alignments. The *PhastCons100* and *PhyloP100way* scores as well as the *multiz100way* alignments for the hg38 human reference genome are available at <https://hgdownload.cse.ucsc.edu/goldenpath/hg38/>.

In the third method (*ProtProf*), we calculated the frequencies of the wild-type and mutant residues in the mutated sites for each mutation. These frequencies are derived from the *BLAST* (Altschul et al. 1997) search alignments against the *UniRef90* database (Suzek et al. 2007) released in June 2020. For the *BLAST* search we used an e-value cutoff of  $10^{-9}$  as suggested in previous works (Capriotti et al. 2006, 2013, 2017; Calabrese et al. 2009). By definition, the E-value represents the number of expected hits found by chance and depends on the number of sequences in the database. In our case, selecting an E-value threshold of  $10^{-9}$  for a *BLAST* search on *UniRef90*, which contains  $\sim 10^8$  sequences, ensures that less than one random hit can be found by chance from our search.

In summary, for each mutated loci, we considered the *PhastCons100way* (*PC*) and *PhyloP10way* (*PP*), the frequencies of the reference ( $f_{ref}$ ) and alternative ( $f_{alt}$ ) alleles from the *multiz100way* multiple sequence alignment, and the total number of aligned genomic sequences ( $N_g$ ). For the protein-based method the protein-sequence profile was obtained considering the sequences returned by *BLAST*. For each mutated site, we calculated the frequencies of wild-type ( $f_{wt}$ ) and mutant ( $f_{mut}$ ) residues and the number of aligned proteins ( $N_p$ ). The nucleotide and amino acid frequencies are calculated as follows:

$$f(x_i) = \frac{n(x_i)}{\sum_{i=k} n(x_i)}$$

Where  $n(x_i)$  is the number of the nucleotide or amino acid  $x_i$  in the sequence alignment and  $k$  is equal to 5 (including the generic nucleotide *N*) and 20 for DNA and protein sequences, respectively.  $N_g$  and  $N_p$  represent the denominators of the equation above for DNA and protein sequences, respectively.

#### Machine learning algorithms

Using the eight features described above, we develop three binary classifiers (*PPScore*, *DNAProf*, *ProtProf*) using the following groups of three features:

- **PPScore:** *PhastCons100way* (*PC*) and *PhyloP100way* (*PP*) scores, and number aligned genomic sequences ( $N_g$ ) in *multiz100way*
- **DNAProf:** Frequencies of the reference ( $f_{ref}$ ) and alternative ( $f_{alt}$ ) alleles, and number aligned genomic sequences in *multiz100way* ( $N_g$ ).
- **ProtProf:** Frequencies of the wild-type ( $f_{wt}$ ) and mutant ( $f_{mut}$ ) residues, and number aligned protein sequences ( $N_p$ ) from a *BLAST* search on *UniRef90*.

For each group of features defined above we developed a binary classifier based on the gradient boosting algorithm as implemented in the *scikit-learn* package (Pedregosa, F. et al. 2011). The proposed groups of features are summarized in Table 1.

#### Training and testing procedure

We first evaluated the performance of each method on *CommonClinvar* using a 10-fold cross-validation procedure for a fair evaluation of the proposed method performance. To reduce at the minimum the possible overfitting we mapped each missense variant on the relative protein sequence and we clustered all the sequences using the *blastclust* algorithm (<https://ftp.ncbi.nih.gov/blast/documents/blastclust.html>) with a sequence identity threshold of 25% and a coverage of 50%. Using the clustering based on

sequence similarity we perform a 10-fold cross-validation procedure keeping all the variants belonging to the same cluster in the same subset. A second test is performed considering the *NewClinvar* dataset. In this case the impact of the variants of a given protein are predicted excluding from the training set (*CommonClinvar*) all the variants belonging to proteins of the same cluster. We extracted a balanced set of *Pathogenic* and *Benign* variants from *CommonClinvar* and *NewClinvar* dataset for each test, randomly downscaling the most abundant class. The reported scoring measures for all the methods are averaged over ten randomly selected sets.

### *Benchmarking and performance measures*

To characterize the prediction power of the main features described in this work, for each of them we developed a single feature binary classifier based on a single threshold. For each feature the classification threshold is optimized on the *CommonClinvar* dataset maximizing both the true positive and true negative rates. The optimized threshold is tested in the classification of the *NewClinvar* variant dataset.

Finally, the performances of all the binary classifiers described above are compared with those achieved by the CADD (Rentzsch et al. 2019) and REVEL (Ioannidis et al. 2016). **algorithms. The optimized raw score threshold for the classification of CADD output was calculated on the *CommonClinvar* dataset as binary classifier. The performances of the methods are scored considering two subsets of the *NewClinvar* dataset including the consensus predictions (*Consensus*) and those with at least one predictor in disagreement with the remaining ones (*NotConsensus*).**

All the measures considered for scoring the performance of the methods are defined in Supplementary Materials.

## **Results**

### *Feature analysis and single feature classification*

In the first part of our work, we analyzed the distributions of the main features used for the classification task. We focused on the six conservation features ( $PC$ ,  $PP$ ,  $f_{ref}$ ,  $f_{alt}$ ,  $f_{wt}$ ,  $f_{mut}$ ) comparing their distributions for the subsets of *Pathogenic* and *Benign* variants. The average, median and standard deviation of such distributions are reported in Table S2. As observed in previous works (Kircher et al. 2014; Capriotti and Fariselli 2017) the distribution of the *PhyloP100way* score ( $PP$ ) in mutated loci associated with *Pathogenic* and *Benign* variants are significantly different (Fig. 1). Indeed, the two distributions show median values of 7.5 and 1.5, respectively, with a Kolmogorov-Smirnov distance ( $D_{KS}$ ) of 0.57 (Fig. 1B and Table S2). This distance is greater than the  $D_{KS}$  observed for the *PhastCons100way* score ( $PC$ ).

A higher difference between the distributions of the conservation scores for the subset of *Pathogenic* and *Benign* variants is observed when the frequencies in sequence profile from genomic and proteins are considered. The most remarkable differences are generally detected when comparing the distributions of the frequency of the alternative allele ( $f_{alt}$ ) and the mutant residue ( $f_{mut}$ ) for which the  $D_{KS}$  is ~0.60. Analyzing the frequencies of the reference allele ( $f_{ref}$ ) and wild-type residue ( $f_{wt}$ ) their  $D_{KS}$  is 0.58 and 0.55, respectively (Table S2). The distributions of the four types of frequencies ( $f_{ref}$ ,  $f_{alt}$ ,  $f_{wt}$ , and  $f_{mut}$ ) for the subsets of *Pathogenic* and *Benign* variants are plotted in Fig. 2

This observation agrees with the results obtained in the prediction of *Pathogenic* variants using a classification threshold on a single feature. The classification threshold is optimized on the *CommonClinvar* dataset maximizing both the true positive and negative rates (Table S3). Applying the optimized thresholds on the prediction of the variants in the *NewClinvar* dataset, we found that a simple classifier based on the frequency of the mutant residue extracted from a protein sequence profile achieve 81% overall accuracy (Q2), 0.63 Matthews correlation coefficient (MCC) and an Area Under the Receiver Operating Characteristic Curve (AUC) of 0.86 (Table 2).

According to the previous observation, the *PhastCons100way* score (*PC*) is the least discriminating feature. When using the optimized threshold on the classification of the *NewClinvar* variants, the method based on a single *PC* threshold achieves 74% overall accuracy, 0.49 MCC and 0.75 AUC (Table 2). Slightly lower performances are obtained when the frequencies of the reference allele and the wild-type residue in the sequence profile are considered. In this case the method based on a single  $f_{ref}$  threshold results in 78% Q2, 0.56 MCC and 0.84 AUC. These results can also be observed plotting the Receiving Operating Characteristic (ROC) and Precision-Recall (PR) curves reported in Fig. S2.

#### Assessment of the machine learning methods

Starting from the previous observations, we developed three machine learning approaches based on the different groups of conservation features. The *PPScore* method is based on the *PhastCons100way*, *PhyloP100way* scores representing unique conservation measures not describing the type of nucleotides observed in the mutated loci. The other two methods consider the frequencies of the nucleotides or residues in the original and new sequences that correspond to  $f_{ref}$ ,  $f_{alt}$  and  $f_{wt}$ ,  $f_{mut}$  for *DNAProf* and *ProtProf*, respectively. To these groups of measures, we added a third feature representing the total number of sequences aligned in the mutated loci ( $N_g$ ,  $N_p$ ). **Although these values are not related to the conservation, they are considered as features for differentiating cases of mutated loci aligned with low and high number of sequences.** We implemented three machine learning methods for predicting *Pathogenic* variants based on the gradient boosting algorithm with these groups of features. First, the performance of these methods is tested with a 10-fold cross-validation procedure on the *CommonClinvar* dataset. To avoid possible overfitting, we clustered all the proteins based on the sequence identity and grouped all their variants in a unique subset. The average performance of *PPScore*, *DNAProf* and *ProtProf* on a balanced set of *Pathogenic* and *Benign* variants are reported in Table S4. The results show that among the three methods *ProtProf*, which is based on protein sequence profile, achieved the highest performance reaching 83% overall accuracy (Q2), 0.67 Matthews correlation coefficient and 0.91 Area Under the Receiver Operating Characteristic Curve (AUC). *PPScore* which is based on *PhastCons100way*, *PhyloP100way* show the lowest performance resulting in ~4% lower AUC and ~9% lower MCC. An intermediate level of performance is achieved by *DNAProf* which results in ~2% lower AUC and ~3% lower MCC with respect to *ProtProf*. Similar results are obtained when assessing the performance of the three methods on the *NewClinvar* dataset. Also, in this case we predicted the impact of each variant removing from the training set all the variants in the *CommonClinvar* training set belonging to the same cluster of proteins. The performance of *PPScore*, *DNAProf* and *ProtProf* on a balanced set of variants from the *NewClinvar* dataset are summarized in Table 3. **For scoring the contribution of  $N_g$  and  $N_p$  to the predictions of the three methods, we removed such features from the input and compared their performances. The results reported in Table S5 show that the methods improve their performance by ~1% for MCC and AUC indices considering  $N_g$  and  $N_p$  in the input features.**

#### Comparison with CADD and REVEL algorithms

In the final part of our analysis we compared the performance of our simple gradient boosting-based algorithms with those obtained with CADD (Rentzsch et al. 2019) and REVEL (Ioannidis et al. 2016). **REVEL (Rare Exome Variant Ensemble Learner) is an ensemble method for predicting the pathogenicity of missense variants on the basis of 13 individual tools. When tested on independent test sets, REVEL shows the best overall performance as compared to any of the individual tools and 7 previously developed ensemble methods.** CADD is one of the most accurate and popular methods for predicting *Pathogenic* variants in coding and non-coding regions (Benevenuta et al. 2021). This method, which is based on more than hundreds of genomic features, was trained on more than 30 million variants. To use CADD as a binary classifier we considered the raw output of the program and we selected the threshold



that maximizes the true positive and negative rates on the *CommonClinvar* dataset. The performance of CADD at the optimal raw score classification threshold of 3.1 is reported in Table S4. This threshold was used for the classification of the variants in the *NewClinvar* dataset. The performances of CADD and REVEL on the *NewClinvar* dataset are summarized in Table 3. This analysis shows that CADD and ProtProf algorithms result in a similar performance in the classification of Pathogenic missense variants in terms of Area Under the Receiver Operating Characteristic (AUC) and Precision-Recall (AUP) curves on both *CommonClinvar* and *NewClinvar* datasets. As expected REVEL outperforms ProtProf and CADD reaching ~3% higher overall accuracy (Q2) and AUC. We can also observe that DNAProf which is based on the sequence profile extracted from the *multiz100way* sequence alignments results only in ~3% lower AUC and AUP. The Receiver Operating Characteristic and Precision-Recall curves for CADD, REVEL and the three methods presented in this manuscript are plotted in Fig. 3.

#### Analysis and comparison of the predictions

To better understand the difference among the presented methods, we compared the predictions of three gradient boosting-based algorithms (PPScore, DNAProf and ProtProf). For performing this analysis, we defined two subsets of the *NewClinvar* dataset: the *Consensus* subset where the three predictions agree and the *NotConsensus* subset where the predictions differ. When performing such comparison, we observe that predictions overlap in ~73% of the cases in the *NewClinvar* dataset (Fig. 4A), while in the remaining 23% a single predictor differs from the other.

ProtProf and DNAProf provide the highest prediction similarity, agreeing in 88% of the cases with a correlation of 0.75 (Fig. 4C). In terms of performance, when focusing on the *Consensus* subset, the performance of ProtProf reaches 0.91 AUC and 0.81 Matthews correlation, while on the remaining subset, all the methods show an AUC<0.65 and PPScore results on AUC<0.5 (Table 4). The decrease in the performance can be explained by comparing the distribution of the frequencies of the wild-type and mutant residues on the *Consensus* and *NotConsensus* subsets. Indeed, the Kolmogorov-Smirnov distance ( $D_{KS}$ ) of the distributions of *fwt* and *fmut* decrease by ~50% when considering the *NotConsensus* subset (Fig. 5).

A similar analysis is performed comparing the predictions of ProtProf, CADD and REVEL. Here the predictions of the three algorithms overlap in ~75% of the cases (Fig. 4B) with an average of ~83% of common predictions and a correlation of ~0.68 for pairwise comparison (Fig. 4D). The performance of the methods on the *Consensus* subsets achieves ~95% in terms of overall accuracy and ~0.95 AUC, while for the *NotConsensus* subset, the performance of CADD and ProtProf are similar to those of a random predictor. REVEL shows the best performance on this subset of the *NewClinvar* dataset, achieving 67% Q2 and 0.68 AUC (Table 5).

The analysis of the distributions of *fwt* and *fmut* on shows a  $D_{KS}$ >0.70 for the *Consensus* subset, while for the *NotConsensus* it drops below 0.2 with both the distributions of the *fwt* and *fmut* for Benign and Pathogenic variants strongly overlapping (Fig. 6).

## Conclusion and discussion

Here we analyzed different evolutionary information encodings for missense variant pathogenicity predictions. We compared the encoding at DNA and protein levels, where different multiple alignments techniques apply. The multiple sequence alignment includes a larger number of proteins and more remote homologs for many genes than pre-calculated genome alignments from the UCSC genome browser. This condition can be the reason why the performance of a method trained using the protein-based information is slightly better. Thus, at least for the missense variants, an input based on evolutionary information of the wild-type and mutated residue performs better than evolutionary measures based on DNA sequence alignment in the prediction of pathogenic variants. Indeed, on the

~27% of the variants on which the predictions of our gradient boosting algorithms disagree, *ProtProf* reaches 6% high overall accuracy and 9% higher AUC with respect to *DNAProf* which rely on precalculated DNA sequence alignment from UCSC.

With these simple inputs based on evolutionary information, a machine learning method can perform comparably to CADD, which uses more sophisticated inputs. When compared with an ensemble-based approach (RAVEL), our basic method (*ProtProf*) results in ~3% lower overall accuracy and AUC. Nevertheless, our analysis based on the comparison of the predictions of different methods allows the identification of a more reliable subset of predictions on which *ProtProf* reaches an overall accuracy above 90% and AUC>0.9.

Recently, it has been suggested that protein positions have a significant role and can act as *Neutral*, *Toggle* or *Rheostat* (Miller et al. 2019). Here we indicate an alternative view of protein positions that can be seen as a non-linear combination of the frequencies of wild-type/mutant residues at protein level or reference/alternative allele at DNA level. The results of our analysis suggest that the performances of new and more sophisticated machine learning algorithms should always be compared with those achieved by simple conservation-based methods. As recently proposed (Walsh et al. 2021), the design of such benchmark tests should consider the adoption of specific guidelines for avoiding bias in the training and testing sets. This procedure is important to exclude overfitting on the context-dependent features (Grimm et al. 2015) and identify new important features for improving the performance of variant scoring algorithms.



## **Declarations**

### *Funding*

This work was supported by the PRIN project, “Integrative tools for defining the molecular basis of the diseases: Computational and Experimental methods for Protein Variant Interpretation” of the Ministero Istruzione, Università e Ricerca (PRIN201744NR8S).

### *Conflicts of interest/Competing interests*

None

### *Availability of data and material*

Additional information is available in Supplementary Materials. The *CommonClinvar* and *NewClinvar* datasets are provided as supplementary files and available at <https://doi.org/10.5281/zenodo.5722031>.

### *Authors' contributions*

EC developed and collected and analyzed the data. Both the authors designed the research and contributed to the writing of the manuscript.

### *Acknowledgments*

PF thanks the Italian Ministry for Education, University and Research for the programme “Dipartimenti di Eccellenza 20182022D15D18000410001”.

## References

- Altschul SF, Madden TL, Schaffer AA, et al (1997) Gapped BLAST and PSI-BLAST: a new generation of protein database search programs. *Nucleic Acids Res* 25:3389–402
- Ancien F, Pucci F, Godfroid M, Romain M (2018) Prediction and interpretation of deleterious coding variants in terms of protein structural stability. *Sci Rep* 8:4480. <https://doi.org/10.1038/s41598-018-22531-2>
- Benevenuta S, Capriotti E, Fariselli P (2021) Calibrating variant-scoring methods for clinical decision making. *Bioinformatics* btaa943. <https://doi.org/10.1093/bioinformatics/btaa943>
- Calabrese R, Capriotti E, Fariselli P, et al (2009) Functional annotations improve the predictive score of human disease-related mutations in proteins. *Hum Mutat* 30:1237–44. <https://doi.org/10.1002/humu.21047>
- Capra JA, Singh M (2007) Predicting functionally important residues from sequence conservation. *Bioinformatics* 23:1875–1882. <https://doi.org/10.1093/bioinformatics/btm270>
- Capriotti E, Calabrese R, Casadio R (2006) Predicting the insurgence of human genetic diseases associated to single point protein mutations with support vector machines and evolutionary information. *Bioinformatics* 22:2729–34. <https://doi.org/10.1093/bioinformatics/btl423>
- Capriotti E, Calabrese R, Fariselli P, et al (2013) WS-SNPs&GO: a web server for predicting the deleterious effect of human protein variants using functional annotation. *BMC Genomics* 14 Suppl 3:S6. <https://doi.org/10.1186/1471-2164-14-S3-S6>
- Capriotti E, Fariselli P (2017) PhD-SNPg: a webserver and lightweight tool for scoring single nucleotide variants. *Nucleic Acids Res* 45:W247–W252. <https://doi.org/10.1093/nar/gkx369>
- Capriotti E, Martelli PL, Fariselli P, Casadio R (2017) Blind prediction of deleterious amino acid variations with SNPs&GO. *Hum Mutat* 38:1064–1071. <https://doi.org/10.1002/humu.23179>
- Capriotti E, Nehrt NL, Kann MG, Bromberg Y (2012) Bioinformatics for personal genome interpretation. *Brief Bioinform* 13:495–512. <https://doi.org/10.1093/bib/bbr070>
- Capriotti E, Ozturk K, Carter H (2019) Integrating molecular networks with genetic variant interpretation for precision medicine. *Wiley Interdiscip Rev Syst Biol Med* 11:e1443. <https://doi.org/10.1002/wsbm.1443>
- Claussnitzer M, Cho JH, Collins R, et al (2020) A brief history of human disease genetics. *Nature* 577:179–189. <https://doi.org/10.1038/s41586-019-1879-7>
- Fernald GH, Capriotti E, Daneshjou R, et al (2011) Bioinformatics challenges for personalized medicine. *Bioinformatics* 27:1741–8. <https://doi.org/10.1093/bioinformatics/btr295>
- Grimm DG, Azencott C, Aicheler F, et al (2015) The Evaluation of Tools Used to Predict the Impact of Missense Variants Is Hindered by Two Types of Circularity. *Hum Mutat* 36:513–523. <https://doi.org/10.1002/humu.22768>
- Ioannidis NM, Rothstein JH, Pejaver V, et al (2016) REVEL: An Ensemble Method for Predicting the Pathogenicity of Rare Missense Variants. *Am J Hum Genet* 99:877–885. <https://doi.org/10.1016/j.ajhg.2016.08.016>
- Kent WJ, Sugnet CW, Furey TS, et al (2002) The human genome browser at UCSC. *Genome Res* 12:996–1006. <https://doi.org/10.1101/gr.229102>
- Kircher M, Witten DM, Jain P, et al (2014) A general framework for estimating the relative pathogenicity of human genetic variants. *Nat Genet* 46:310–5. <https://doi.org/10.1038/ng.2892>
- Landrum MJ, Chitipiralla S, Brown GR, et al (2020) ClinVar: improvements to accessing data. *Nucleic Acids Res* 48:D835–D844. <https://doi.org/10.1093/nar/gkz972>
- MacArthur DG, Manolio TA, Dimmock DP, et al (2014) Guidelines for investigating causality of sequence variants in human disease. *Nature* 508:469–76.

- <https://doi.org/10.1038/nature13127>
- McInnes G, Sharo AG, Koleske ML, et al (2021) Opportunities and challenges for the computational interpretation of rare variation in clinically important genes. *Am J Hum Genet* 108:535–548. <https://doi.org/10.1016/j.ajhg.2021.03.003>
- Miller M, Vitale D, Kahn PC, et al (2019) funtrp: identifying protein positions for variation driven functional tuning. *Nucleic Acids Res* 47:e142. <https://doi.org/10.1093/nar/gkz818>
- Niroula A, Vihinen M (2016) Variation Interpretation Predictors: Principles, Types, Performance, and Choice. *Hum Mutat* 37:579–597. <https://doi.org/10.1002/humu.22987>
- Ozturk K, Carter H (2021) Predicting functional consequences of mutations using molecular interaction network features. *Hum Genet*. <https://doi.org/10.1007/s00439-021-02329-5>
- Pedregosa, F., Varoquaux, G., Gramfort, A., et al (2011) Scikit-learn: Machine Learning in Python. *JMLR* 12:2825–2830
- Petrosino M, Novak L, Pasquo A, et al (2021) Analysis and Interpretation of the Impact of Missense Variants in Cancer. *Int J Mol Sci* 22:5416. <https://doi.org/10.3390/ijms22115416>
- Pollard KS, Hubisz MJ, Rosenbloom KR, Siepel A (2010) Detection of nonneutral substitution rates on mammalian phylogenies. *Genome Res* 20:110–21. <https://doi.org/gr.097857.109> [pii] 10.1101/gr.097857.109
- Rentzsch P, Witten D, Cooper GM, et al (2019) CADD: predicting the deleteriousness of variants throughout the human genome. *Nucleic Acids Res* 47:D886–D894. <https://doi.org/10.1093/nar/gky1016>
- Rost B, Radivojac P, Bromberg Y (2016) Protein function in precision medicine: deep understanding with machine learning. *FEBS Lett* 590:2327–2341. <https://doi.org/10.1002/1873-3468.12307>
- Schneider TD (1997) Information content of individual genetic sequences. *J Theor Biol* 189:427–441. <https://doi.org/10.1006/jtbi.1997.0540>
- Siepel A, Bejerano G, Pedersen JS, et al (2005) Evolutionarily conserved elements in vertebrate, insect, worm, and yeast genomes. *Genome Res* 15:1034–50. <https://doi.org/gr.3715005> [pii] 10.1101/gr.3715005
- Suzek BE, Huang H, McGarvey P, et al (2007) UniRef: comprehensive and non-redundant UniProt reference clusters. *Bioinformatics* 23:1282–8. <https://doi.org/btm098> [pii] 10.1093/bioinformatics/btm098
- Tennessen JA, Bigham AW, O'Connor TD, et al (2012) Evolution and functional impact of rare coding variation from deep sequencing of human exomes. *Science* 337:64–69. <https://doi.org/10.1126/science.1219240>
- Valdar WSJ (2002) Scoring residue conservation. *Proteins* 48:227–241. <https://doi.org/10.1002/prot.10146>
- Walsh I, Fishman D, Garcia-Gasulla D, et al (2021) DOME: recommendations for supervised machine learning validation in biology. *Nat Methods*. <https://doi.org/10.1038/s41592-021-01205-4>

## Tables

| Group                  | Features  |           |       |
|------------------------|-----------|-----------|-------|
| <b><i>PPScore</i></b>  | <i>PC</i> | <i>PP</i> | $N_g$ |
| <b><i>DNAProf</i></b>  | $f_{ref}$ | $f_{alt}$ | $N_g$ |
| <b><i>ProtProf</i></b> | $f_{wt}$  | $f_{mut}$ | $N_p$ |

**Table 1:** Three groups of features used for the development of the binary classifiers.

| Feature   | Threshold | Q2    | TNR   | NPV   | TPR   | PPV   | MCC   | F1    | AUC   | AUP   |
|-----------|-----------|-------|-------|-------|-------|-------|-------|-------|-------|-------|
| <i>PC</i> | 1.000     | 0.737 | 0.611 | 0.816 | 0.862 | 0.689 | 0.489 | 0.766 | 0.755 | 0.815 |
| <i>PP</i> | 4.704     | 0.769 | 0.796 | 0.756 | 0.743 | 0.784 | 0.539 | 0.763 | 0.841 | 0.828 |
| $f_{ref}$ | 0.977     | 0.779 | 0.815 | 0.760 | 0.742 | 0.801 | 0.559 | 0.770 | 0.836 | 0.843 |
| $f_{alt}$ | 0.000     | 0.794 | 0.750 | 0.821 | 0.837 | 0.770 | 0.589 | 0.802 | 0.828 | 0.863 |
| $f_{wt}$  | 0.702     | 0.769 | 0.806 | 0.750 | 0.731 | 0.791 | 0.539 | 0.759 | 0.844 | 0.836 |
| $f_{mut}$ | 0.005     | 0.815 | 0.819 | 0.812 | 0.810 | 0.817 | 0.629 | 0.814 | 0.857 | 0.856 |

**Table 2.** Performance of basic predictors based on a single feature on the *NewClinvar* dataset. Prediction threshold are optimized on the *CommonClinvar* dataset. Q2: Overall Accuracy, TNR: True negative rate, NPV: Negative predicted value, TPR: True Positive Rate, PPV: Positive Predicted Value, MCC: Matthews Correlation Coefficient, F1: harmonic mean of precision and sensitivity, AUC: Area Under the Receiver Operator Characteristic Curve, AUP Area under the Precision Recall Curve. All the performance measures are defined in Supplementary Materials.

| Method   | Q2    | TNR   | NPV   | TPR   | PPV   | MCC   | F1    | AUC   | AUP   |
|----------|-------|-------|-------|-------|-------|-------|-------|-------|-------|
| CADD     | 0.844 | 0.821 | 0.860 | 0.867 | 0.829 | 0.688 | 0.847 | 0.911 | 0.905 |
| REVEL    | 0.871 | 0.918 | 0.843 | 0.825 | 0.909 | 0.747 | 0.865 | 0.945 | 0.942 |
| ProtProf | 0.831 | 0.865 | 0.809 | 0.796 | 0.855 | 0.662 | 0.824 | 0.910 | 0.905 |
| DNAProf  | 0.812 | 0.780 | 0.834 | 0.845 | 0.794 | 0.626 | 0.818 | 0.881 | 0.873 |
| PPScore  | 0.771 | 0.776 | 0.769 | 0.767 | 0.774 | 0.543 | 0.770 | 0.855 | 0.846 |

**Table 3: Testing prediction on** the *NewClinvar* variant dataset. Q2: Overall Accuracy, TNR: True negative rate, NPV: Negative predicted value, TPR: True Positive Rate, PPV: Positive Predicted Value, MCC: Matthews Correlation Coefficient, F1: harmonic mean of precision and sensitivity, AUC: Area Under the Receiver Operator Characteristic Curve, AUP Area Under the Precision Recall Curve. All the performance measures are defined in Supplementary Materials. For CADD a raw score classification threshold of 3.1 was considered.

| Method   | Subset       | Q2    | TNR   | NPV   | TPR   | PPV   | MCC    | F1    | AUC   | AUP   |
|----------|--------------|-------|-------|-------|-------|-------|--------|-------|-------|-------|
| ProtProf | Consensus    | 0.905 | 0.907 | 0.909 | 0.904 | 0.901 | 0.810  | 0.902 | 0.905 | 0.929 |
| ProtProf | NotConsensus | 0.633 | 0.740 | 0.577 | 0.542 | 0.712 | 0.286  | 0.615 | 0.641 | 0.735 |
| DNAProf  | NotConsensus | 0.567 | 0.402 | 0.536 | 0.706 | 0.583 | 0.113  | 0.639 | 0.554 | 0.665 |
| PPScore  | NotConsensus | 0.418 | 0.385 | 0.369 | 0.445 | 0.461 | -0.170 | 0.453 | 0.415 | 0.561 |

**Table 4.** Performance of *PPScore*, *DNAProf* and *ProtProf* on two subsets of the *NewClinvar* dataset. *Consensus*: Subset of *NewClinvar* (72.6%) for which the predictions of the three methods are in agreement. *NotConsensus*: subset of *NewClinvar* (27.4%) for which one method differs from the remaining two. Q2: Overall Accuracy, TNR: True negative rate, NPV: Negative predicted value, TPR: True Positive Rate, PPV: Positive Predicted Value, MCC: Matthews Correlation Coefficient, F1: harmonic mean of precision and sensitivity, AUC: Area Under the Receiver Operator Characteristic Curve, AUP Area Under the Precision Recall Curve. All the performance measures are defined in Supplementary Materials.

| Method          | Subset              | Q2    | TNR   | NPV   | TPR   | PPV   | MCC    | F1    | AUC   | AUP   |
|-----------------|---------------------|-------|-------|-------|-------|-------|--------|-------|-------|-------|
| <i>ProtProf</i> | <i>Consensus</i>    | 0.945 | 0.954 | 0.941 | 0.935 | 0.950 | 0.890  | 0.943 | 0.945 | 0.959 |
| <i>ProtProf</i> | <i>NotConsensus</i> | 0.479 | 0.539 | 0.429 | 0.431 | 0.541 | -0.029 | 0.480 | 0.485 | 0.616 |
| REVEL           | <i>NotConsensus</i> | 0.662 | 0.777 | 0.589 | 0.570 | 0.763 | 0.350  | 0.653 | 0.674 | 0.760 |
| CADD            | <i>NotConsensus</i> | 0.531 | 0.337 | 0.458 | 0.684 | 0.565 | 0.022  | 0.619 | 0.510 | 0.628 |

**Table 5.** Performance of REVEL, CADD and *ProtProf* on two subsets of the NewClinvar dataset. *Consensus*: Subset of *NewClinvar* (75.5%) for which the predictions of the three methods are in agreement. *NotConsensus*: subset of *NewClinvar* (24.5%) for which one method differs from the remaining two. Q2: Overall Accuracy, TNR: True negative rate, NPV: Negative predicted value, TPR: True Positive Rate, PPV: Positive Predicted Value, MCC: Matthews Correlation Coefficient, F1: harmonic mean of precision and sensitivity, AUC: Area Under the Receiver Operator Characteristic Curve, AUP Area Under the Precision Recall Curve. All the performance measures are defined in Supplementary Materials.



## Figures

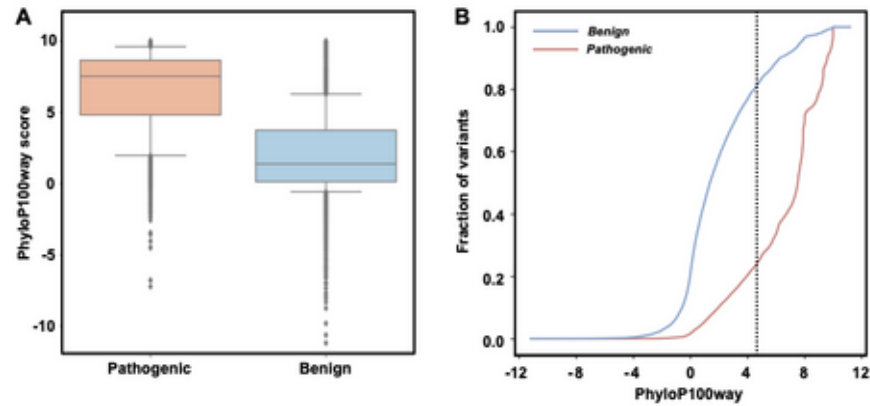


**Figure 1.** (A) Box plot and (B) cumulative distributions of the *PhyloP100way* score in the variation sites for the subsets of *Pathogenic* and *Benign* variants in the *CommonClinvar* dataset. The maximum distance between the two distributions is at 4.7 that corresponds to a Kolmogorov Smirnov distance of 0.57.

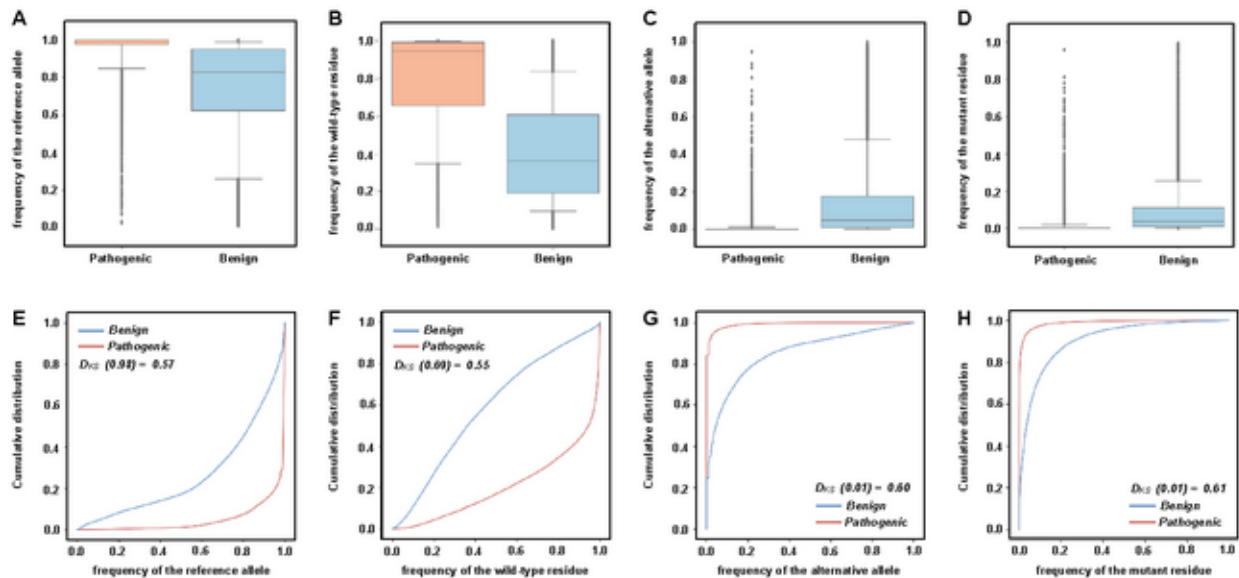


**Figure 2.** Box plots and cumulative distributions of the frequencies of references (A,E) / alternative (C,F) alleles in the variation sites and the frequencies of wild-type (B,G) / mutant (D,H) residues in protein mutation sites for the subset of *Pathogenic* and *Benign* variants in the *CommonClinvar* dataset. In the cumulative distribution plot (E,F,G,H) is reported the Kolmogorov-Smirnov distance ( $D_{KS}$ ) which represents the maximum distance between the distributions of the frequencies for Pathogenic and Benign variants.

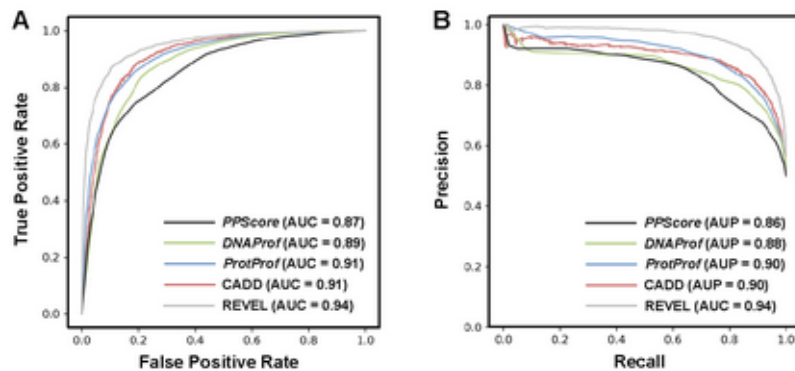


**Figure 3.** Receiver Operating Characteristic (A) and Precision Recall (B) curves for the different gradient boosting algorithms (PPScore, DNAProf, ProtProf), CADD and REVEL on the NewClinvar dataset.

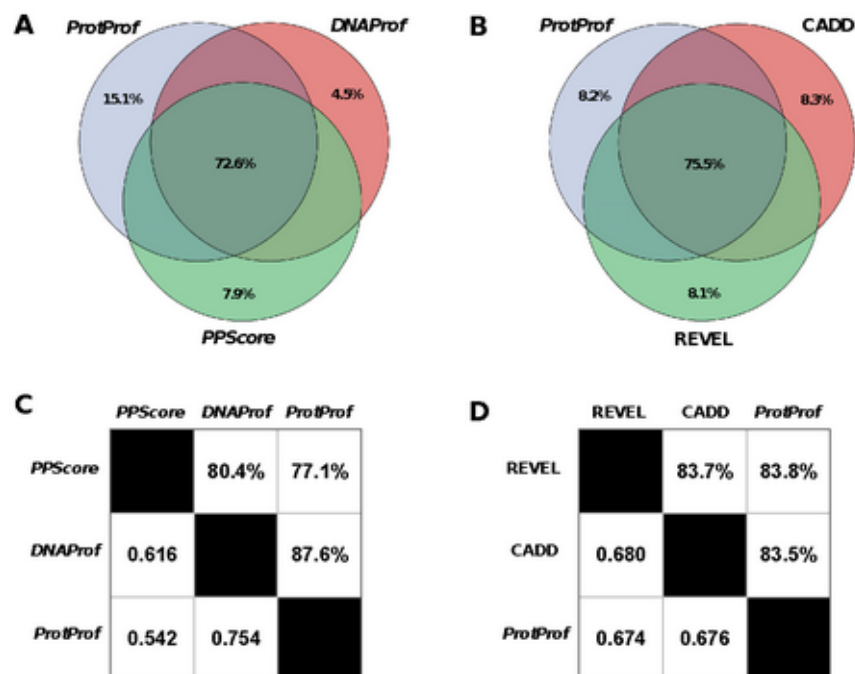


**Figure 4.** Overlap of the predictions of the different methods on the NewClinvar dataset. (A) Venn diagram of the prediction of the 3 gradient boosting algorithms (PPScore, DNAProf, ProtProf) and (B) Venn diagram of the prediction of ProtProf, CADD and REVEL. (C) Pairwise overlap of the prediction of the 3 gradient boosting algorithms and (D) Pairwise overlap of the prediction of the ProtProf, CADD and REVEL. The numbers above the diagonal represent the fraction of common predictions while those below the diagonal are the correlations between the predictions.

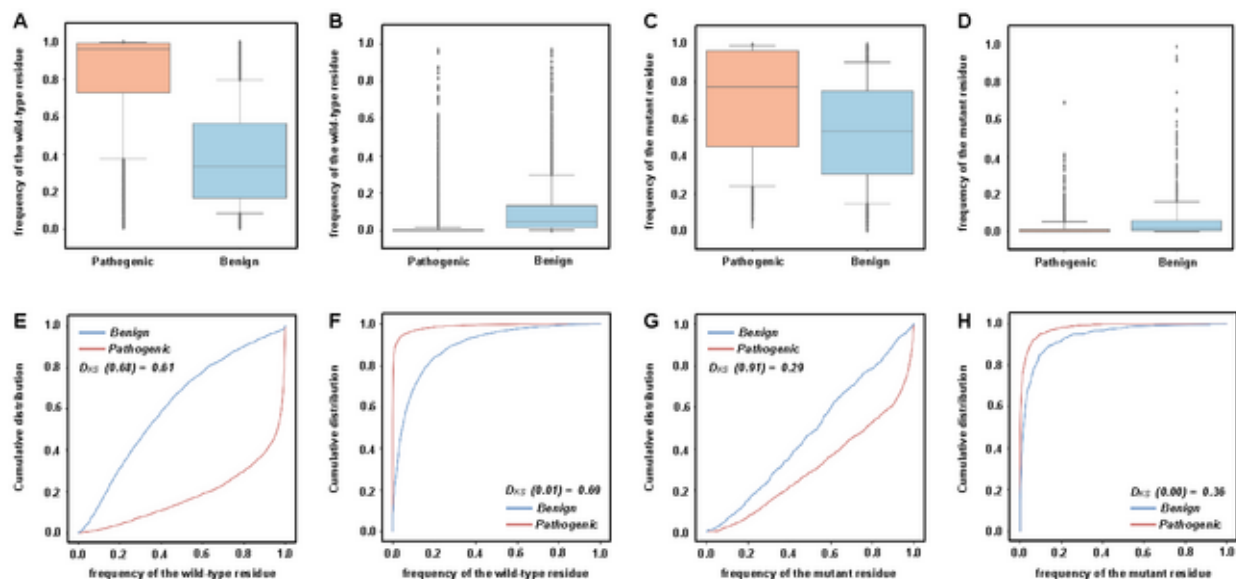


**Figure 5.** Box plots and cumulative distributions of the frequencies of wild-type and mutant residues subset of *NewClinvar* for which the predictions of *PPScore*, *DNAProf* and *ProtProf* are in agreement (A,B,E,F) or in disagreement (C,D,G,H). In the cumulative distribution plot (E,F,G,H) is reported the Kolmogorov-Smirnov distance ( $D_{KS}$ ) which represents the maximum distance between the distributions of the frequencies for Pathogenic and Benign variants. Average and standard deviations of the distributions are reported in Table S6.

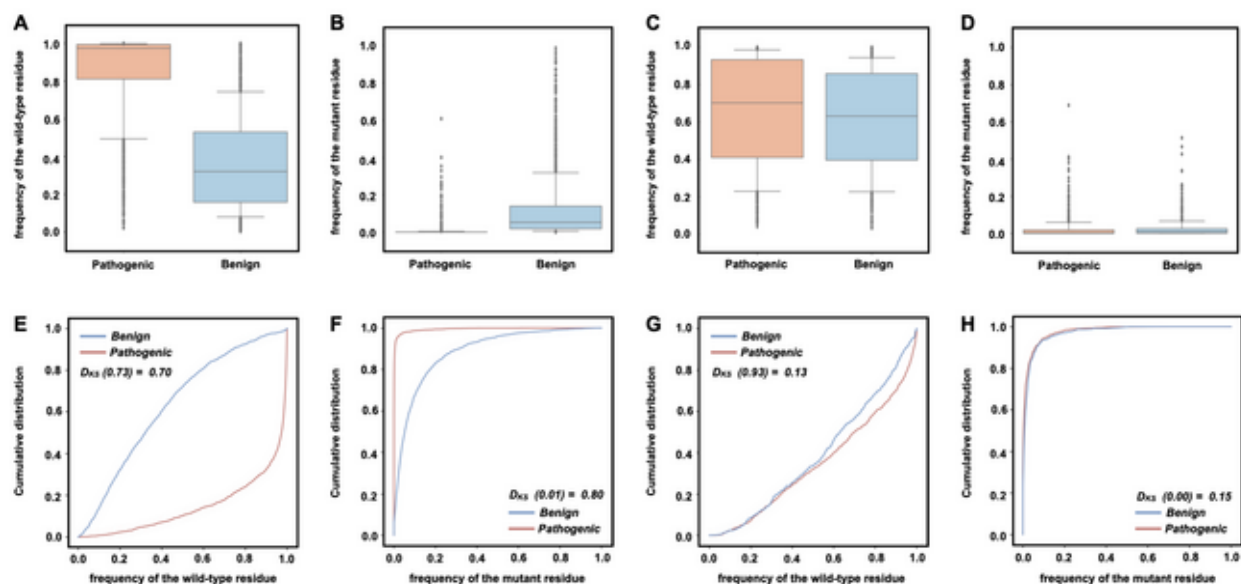


**Figure 6.** Box plots and cumulative distributions of the frequencies of wild-type and mutant residues subset of *NewClinvar* for which the predictions of *REVEL*, *CADD* and *ProtProf* are in agreement (A,B,E,F) or in disagreement (C,D,G,H). In the cumulative distribution plot (E,F,G,H) is reported the Kolmogorov-Smirnov distance ( $D_{KS}$ ) which represents the maximum distance between the distributions of the frequencies for Pathogenic and Benign variants. Average and standard deviations of the distributions are reported in Table S7.

## SUPPLEMENTARY MATERIALS

### Evaluating the relevance of sequence conservation in the prediction of pathogenic missense variants

Emidio Capriotti<sup>1\*</sup> and Piero Fariselli<sup>2\*</sup>

<sup>1</sup> BioFold Unit, Department of Pharmacy and Biotechnology (FaBiT), University of Bologna,  
Via F. Selmi 3, 40126 Bologna, Italy.

<sup>2</sup> Department of Medical Sciences, University of Torino,  
Via Santena 19, 10126, Torino, Italy.

Contacts: [emidio.capriotti@unibo.it](mailto:emidio.capriotti@unibo.it), [piero.fariselli@unito.it](mailto:piero.fariselli@unito.it)

#### Performance measures for binary classifiers

For each prediction, the binary classification (*Pathogenic/Benign*) is made at the threshold  $t$ . Thus, if a selected score for *Pathogenic* classification is  $>t$  the variant is predicted to be *Pathogenic*. For single feature-based predictors the classification threshold is optimized on the *CommonClinvar* dataset (Table S2) while for the gradient boosting algorithm and REVEL (Ioannidis *et al.* 2016) the output threshold is set to 0.5. For CADD (Rentzsch *et al.* 2019) a raw score threshold of 3.1 was used to calculate the performance.

In all the performance measures - assuming that positives indicate *Pathogenic* and negatives indicate *Benign* - TP (true positives) are correctly predicted Pathogenic Single Nucleotide Variants (SNVs), TN (true negatives) are correctly predicted *Benign* variants, FP (false positives) *Benign* SNVs annotated as *Pathogenic*, and FN (false negatives) are *Pathogenic* variants predicted to be *Benign*. Predictor performance was evaluated using the following metrics: true positive and negative rates ( $TPR$ ,  $TNR$ ), positive and negative predicted values ( $PPV$ ,  $NPV$ ),  $F1$  score and overall accuracy ( $Q_2$ )

$$\begin{aligned} PPV &= \frac{TP}{TP + FP} & TPR &= \frac{TP}{TP + FN} \\ NPV &= \frac{TN}{TN + FN} & TNR &= \frac{TN}{TN + FP} \\ F1 &= \frac{2TP}{2TP + FP + FN} & Q_2 &= \frac{TP + TN}{TP + FP + TN + FN} \end{aligned} \quad [\text{Eq. 1}]$$

We computed the Matthew's correlation coefficient MCC (Eq. 2) as:

$$MCC = \frac{TP \times TN - FP \times FN}{\sqrt{(TP + FP)(TP + FN)(TN + FP)(TN + FN)}} \quad [\text{Eq. 2}]$$

We also calculated the area under the receiver operating characteristic (ROC) curve (AUC), by plotting the True Positive Rate as a function of the False Positive Rate and the Area and the Precision Recall Curve (AUP) at different probability thresholds of annotating a variant as *Pathogenic* or *Benign*. Sensitivity = Recall = TPR, Precision = PPV.

For each method, the reported scoring measures are obtained averaging the performance on ten randomly selected sets from *CommonClinvar* and *NewClinvar* datasets. The selection procedure is performed for generating balanced datasets of Pathogenic and Benign variants downscaling the most abundant class of variants.

## Supplementary Tables

| Dataset              | Annotation        | Proteins | Mutations      |
|----------------------|-------------------|----------|----------------|
| <i>CommonClinvar</i> | All               | 7,582    | 36,751         |
|                      | <i>Benign</i>     | 6,444    | 19,659 (53.5%) |
|                      | <i>Pathogenic</i> | 3,117    | 17,092 (46.5%) |
| <i>NewClinvar</i>    | All               | 1,855    | 5,172          |
|                      | <i>Benign</i>     | 935      | 2,247 (43.4%)  |
|                      | <i>Pathogenic</i> | 1,119    | 2,925 (56.6%)  |

**Table S1.** Composition of the datasets extracted from *Clinvar* database (<https://www.ncbi.nlm.nih.gov/clinvar/>),



| Dataset              | Feature<br>s | $D_{KS}$ | Pathogenic |        |       | Benign |        |       |
|----------------------|--------------|----------|------------|--------|-------|--------|--------|-------|
|                      |              |          | Mean       | Median | Std   | Mean   | Median | Std   |
| <b>CommonClinvar</b> | <i>PC</i>    | 0.529    | 0.957      | 1.000  | 0.185 | 0.562  | 0.893  | 0.466 |
|                      | <i>PP</i>    | 0.573    | 6.523      | 7.521  | 2.794 | 2.120  | 1.374  | 2.789 |
|                      | $f_{ref}$    | 0.579    | 0.956      | 1.000  | 0.108 | 0.739  | 0.830  | 0.270 |
|                      | $f_{alt}$    | 0.598    | 0.008      | 0.000  | 0.036 | 0.147  | 0.047  | 0.226 |
|                      | $f_{wt}$     | 0.545    | 0.797      | 0.945  | 0.261 | 0.414  | 0.362  | 0.270 |
|                      | $f_{mut}$    | 0.609    | 0.011      | 0.000  | 0.043 | 0.092  | 0.037  | 0.143 |
| <b>NewClinvar</b>    | <i>PC</i>    | 0.473    | 0.951      | 1.000  | 0.198 | 0.598  | 0.966  | 0.460 |
|                      | <i>PP</i>    | 0.548    | 6.461      | 7.509  | 2.861 | 2.301  | 1.521  | 2.782 |
|                      | $f_{ref}$    | 0.563    | 0.953      | 1.000  | 0.109 | 0.734  | 0.836  | 0.283 |
|                      | $f_{alt}$    | 0.590    | 0.008      | 0.000  | 0.037 | 0.159  | 0.047  | 0.244 |
|                      | $f_{wt}$     | 0.546    | 0.802      | 0.943  | 0.257 | 0.420  | 0.378  | 0.273 |
|                      | $f_{mut}$    | 0.632    | 0.010      | 0.000  | 0.038 | 0.096  | 0.037  | 0.148 |

**Table S2.** Statistics of the distribution of six conservation features for the subset of *Pathogenic* and *Benign* variants in the *CommonClinvar* and *NewClinvar* datasets. *PC*: *PhastCons100way* score. *PP*: *PhyloP100way* score,  $f_{ref}$  and  $f_{alt}$ : frequencies of the reference and alternate alleles in the *multiz100way* genomic alignment,  $f_{wt}$  and  $f_{mut}$ : frequencies of the wild-type and mutant residues from a multiple protein sequence alignment.  $D_{KS}$  is the distance between two cumulative distributions calculated through the Kolmogorov-Smirnov test.

|             | Feature Threshold | Q2    | TNR   | NPV   | TPR   | PPV   | MCC   | F1    | AUC   | AUP   |
|-------------|-------------------|-------|-------|-------|-------|-------|-------|-------|-------|-------|
| <i>PCPC</i> | 1.000             | 0.764 | 0.655 | 0.838 | 0.874 | 0.717 | 0.541 | 0.787 | 0.782 | 0.836 |
| <i>PP</i>   | 4.704             | 0.786 | 0.815 | 0.771 | 0.758 | 0.804 | 0.574 | 0.780 | 0.856 | 0.844 |
| $f_{ref}$   | 0.977             | 0.789 | 0.825 | 0.770 | 0.754 | 0.812 | 0.580 | 0.781 | 0.844 | 0.848 |
| $f_{alt}$   | 0.000             | 0.798 | 0.758 | 0.824 | 0.838 | 0.776 | 0.598 | 0.806 | 0.832 | 0.865 |
| $f_{wt}$    | 0.702             | 0.773 | 0.822 | 0.748 | 0.723 | 0.802 | 0.548 | 0.761 | 0.842 | 0.831 |
| $f_{mut}$   | 0.005             | 0.805 | 0.807 | 0.803 | 0.802 | 0.807 | 0.609 | 0.804 | 0.851 | 0.850 |

**Table S3.** Performance of the basic predictors based on a single feature on the *CommonClinvar* dataset. Prediction threshold are optimized maximizing both the True Positive Rate (TPR) and the True Negative Rate (TNR) dataset. Q2: Overall Accuracy, TNR: True negative rate, NPV: Negative predicted value, TPR: True Positive Rate, PPV: Positive Predicted Value, MCC: Matthews Correlation Coefficient, F1: harmonic mean of precision and sensitivity, AUC: Area Under the Receiver Operator Characteristic Curve, AUP Area under the Precision Recall Curve. All the performance measures are defined above.

| Method          | Q2    | TNR   | NPV   | TPR   | PPV   | MCC   | F1    | AUC   | AUP   |
|-----------------|-------|-------|-------|-------|-------|-------|-------|-------|-------|
| CADD            | 0.841 | 0.819 | 0.857 | 0.864 | 0.826 | 0.683 | 0.845 | 0.910 | 0.904 |
| REVEL           | 0.902 | 0.933 | 0.879 | 0.871 | 0.929 | 0.806 | 0.899 | 0.961 | 0.960 |
| <i>ProtProf</i> | 0.833 | 0.868 | 0.811 | 0.798 | 0.858 | 0.667 | 0.827 | 0.906 | 0.901 |
| <i>DNAProf</i>  | 0.821 | 0.791 | 0.842 | 0.851 | 0.803 | 0.644 | 0.827 | 0.888 | 0.879 |
| <i>PPScore</i>  | 0.792 | 0.798 | 0.788 | 0.785 | 0.796 | 0.583 | 0.790 | 0.868 | 0.859 |

**Table S4:** Prediction in cross-validation the *CommonClinvar* dataset. Q2: Overall Accuracy, TNR: True negative rate, NPV: Negative predicted value, TPR: True Positive Rate, PPV: Positive Predicted Value, MCC: Matthews Correlation Coefficient, F1: harmonic mean of precision and sensitivity, AUC: Area Under the Receiver Operator Characteristic Curve, AUP Area under the Precision Recall Curve. For CADD a raw score classification threshold of 3.1 was considered. All the performance measures are defined above.

| Features             | Q2    | TNR   | NPV   | TPR   | PPV   | MCC   | F1    | AUC   | AUP   |
|----------------------|-------|-------|-------|-------|-------|-------|-------|-------|-------|
| <i>PPScore - Ng</i>  | 0.768 | 0.772 | 0.765 | 0.763 | 0.770 | 0.536 | 0.767 | 0.847 | 0.835 |
| <i>PPScore</i>       | 0.771 | 0.776 | 0.769 | 0.767 | 0.774 | 0.543 | 0.770 | 0.855 | 0.846 |
| <i>DNAProf - Ng</i>  | 0.794 | 0.739 | 0.830 | 0.849 | 0.765 | 0.592 | 0.805 | 0.868 | 0.855 |
| <i>DNAProf</i>       | 0.812 | 0.780 | 0.834 | 0.845 | 0.794 | 0.626 | 0.818 | 0.881 | 0.873 |
| <i>ProtProf - Np</i> | 0.827 | 0.829 | 0.825 | 0.824 | 0.829 | 0.654 | 0.827 | 0.895 | 0.888 |
| <i>ProtProf</i>      | 0.831 | 0.865 | 0.809 | 0.796 | 0.855 | 0.662 | 0.824 | 0.910 | 0.905 |

**Table S5.** Testing prediction of the three basic methods (*PPScore*, *DNAProf* and *ProtProf*) excluding *Ng* and *Np* from the features. Q2: Overall Accuracy, TNR: True negative rate, NPV: Negative predicted value, TPR: True Positive Rate, PPV: Positive Predicted Value, MCC: Matthews Correlation Coefficient, F1: harmonic mean of precision and sensitivity, AUC: Area Under the Receiver Operator Characteristic Curve, AUP Area under the Precision Recall Curve. All the performance measures defined above are calculated on the *NewClinvar* dataset.

| Frequency | Subset              | $D_{KS}$ | Pathogenic |       | Benign |       |
|-----------|---------------------|----------|------------|-------|--------|-------|
|           |                     |          | Mean       | Std   | Mean   | Std   |
| $f_{wt}$  | <i>Consensus</i>    | 0.697    | 0.858      | 0.220 | 0.367  | 0.249 |
|           | <i>NotConsensus</i> | 0.133    | 0.657      | 0.285 | 0.614  | 0.266 |
| $f_{mut}$ | <i>Consensus</i>    | 0.798    | 0.005      | 0.030 | 0.114  | 0.158 |
|           | <i>NotConsensus</i> | 0.152    | 0.022      | 0.054 | 0.028  | 0.062 |

**Table S6.** Comparison of the distributions of the frequencies of wild-type and mutant residues on the subset of *NewClinvar* for which the predictions of *PPScore*, *DNAProf* and *ProtProf* are in agreement (*Consensus*) or in disagreement (*NotConsensus*).  $D_{KT}$  is the Kolmogorov-Smirnov distance between the cumulative distributions of the frequencies for Pathogenic and Benign variants.

| Frequency | Subset              | $D_{KS}$ | Pathogenic |       | Benign |       |
|-----------|---------------------|----------|------------|-------|--------|-------|
|           |                     |          | Mean       | Std   | Mean   | Std   |
| $f_{wt}$  | <i>Consensus</i>    | 0.697    | 0.849      | 0.225 | 0.386  | 0.264 |
|           | <i>NotConsensus</i> | 0.133    | 0.692      | 0.290 | 0.525  | 0.273 |
| $f_{mut}$ | <i>Consensus</i>    | 0.798    | 0.006      | 0.030 | 0.108  | 0.154 |
|           | <i>NotConsensus</i> | 0.152    | 0.020      | 0.053 | 0.061  | 0.124 |

**Table S7.** Comparison of the distributions of the frequencies of wild-type and mutant residues on the subset of *NewClinvar* for which the predictions of REVEL, CADD and *ProtProf* are in agreement (*Consensus*) or in disagreement (*NotConsensus*).  $D_{KT}$  is the Kolmogorov-Smirnov distance between the cumulative distributions of the frequencies for Pathogenic and Benign variants.

## Supplementary figures

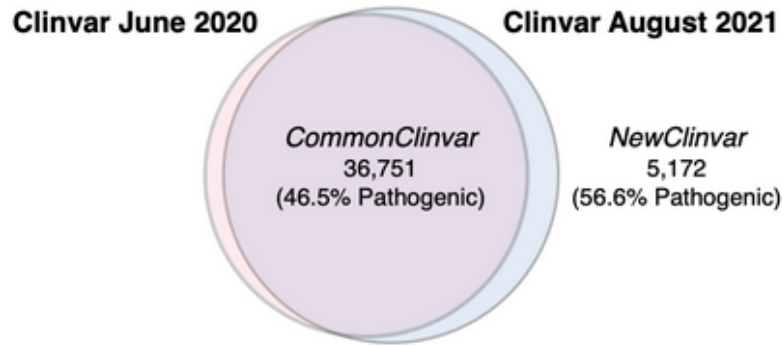


**Figure S1.** Venn diagram showing the intersection and difference between the two versions (August 2021 and June 2020) of Clinvar database (<https://www.ncbi.nlm.nih.gov/clinvar/>) used for generating the *CommonClinvar* and *NewClinvar* datasets

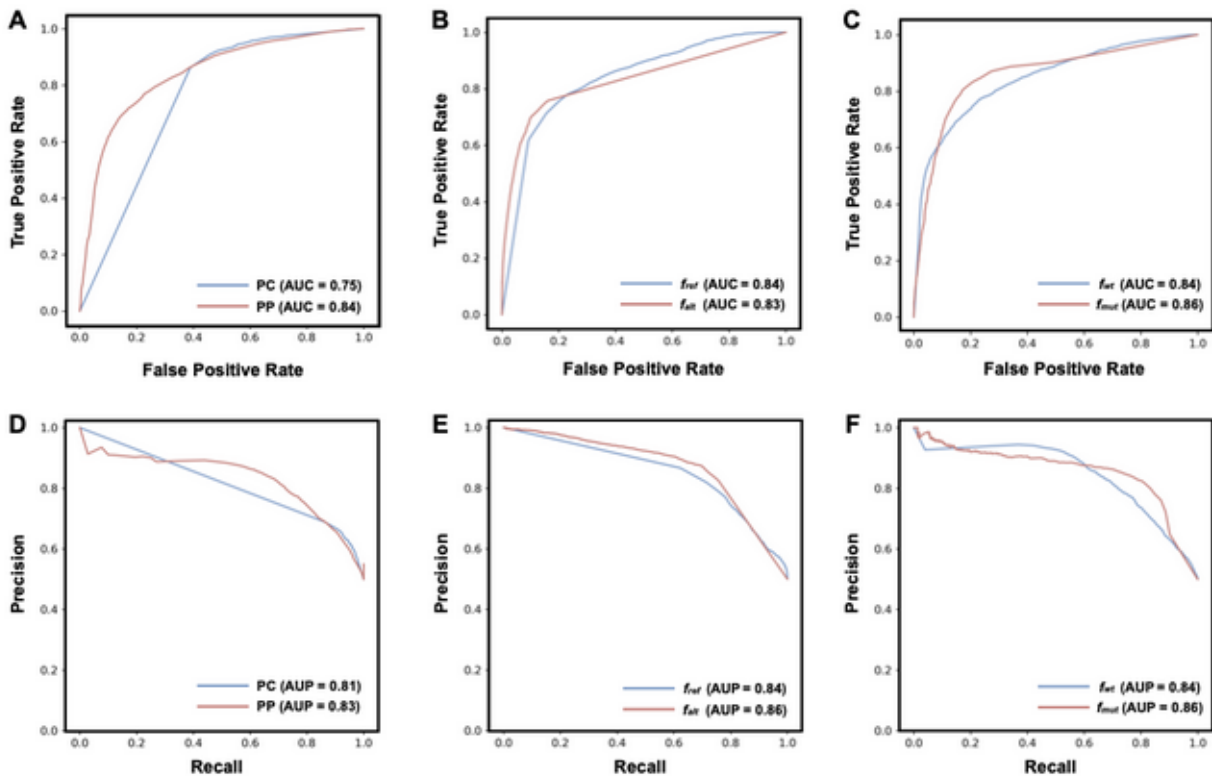


**Figure S2.** Receiver Operating Characteristic (A,B,C) and Precision Recall (D,E,F) curves for single feature predictors on the *NewClinvar* dataset. PC: *PhastCons100way* score. PP: *PhyloP100way* score,  $f_{ref}$  and  $f_{alt}$ : frequencies of the reference and alternate alleles in the *multiz100way* genomic alignment,  $f_{wt}$  and  $f_{mut}$ : frequencies of the wild-type and mutant residues from a multiple protein sequence alignment.

## REFERENCES

- Ioannidis NM, Rothstein JH, Pejaver V, et al (2016) REVEL: An Ensemble Method for Predicting the Pathogenicity of Rare Missense Variants. *Am J Hum Genet* 99:877–885.
- Rentzsch P, Witten D, Cooper GM, et al (2019) CADD: predicting the deleteriousness of variants throughout the human genome. *Nucleic Acids Res* 47:D886–D894.